

PAPER • OPEN ACCESS

Transition from electrostatic to electromagnetic modes of low-frequency fluctuations in RT-1





To cite this article: H. Saitoh *et al* 2024 *Nucl. Fusion* **64** 126011

View the [article online](#) for updates and enhancements.

You may also like

- [Reversed-field-pinch research](#)
H.A.B. Bodin and A.A. Newton
- [Imaging water velocity and volume fraction distributions in water continuous multiphase flows using inductive flow tomography and electrical resistance tomography](#)
Yiqing Meng and Gary P Lucas
- [High- plasma formation and observation of peaked density profile in RT-1](#)
H. Saitoh, Z. Yoshida, J. Morikawa et al.

Transition from electrostatic to electromagnetic modes of low-frequency fluctuations in RT-1

H. Saitoh^{1,2,*} , R. Nakagawa¹, K. Ueda¹, T. Mori¹, M. Nishiura^{1,2} , N. Kenmochi^{2,3} ,
N. Sato²  and Z. Yoshida²

¹ Graduate School of Frontier Sciences, The University of Tokyo, Kashiwa, Japan

² National Institute for Fusion Science, Toki, Japan

³ Graduate Institute for Advanced Studies, The Graduate University for Advanced Studies, SOKENDAI, Toki, Japan

E-mail: saito@ppl.k.u-tokyo.ac.jp

Received 14 January 2024, revised 18 August 2024

Accepted for publication 13 September 2024

Published 26 September 2024



Abstract

We report the electrostatic and electromagnetic behaviors of low-frequency fluctuations and their spatial structures observed in the RT-1 (Ring Trap 1) levitated dipole experiment. By using movable Langmuir probes capable of operating under the high-heat flux conditions, we investigated the spatial structures of electrostatic fluctuations in the plasma and compared them with magnetic fluctuation properties. Low-frequency electrostatic fluctuations in low-beta plasma transact into electromagnetic modes in high-beta operation, the latter of which has been found with edge magnetic probes in previous studies. Multi-point measurements with the Langmuir probes revealed that, in low-beta plasma, the fluctuations propagate in the electron diamagnetic direction and exhibit a toroidal mode number of 3 or 4 in a broad region across different magnetic surfaces. In the high-beta plasma, the phase velocity of the fluctuations has a clear dependence on the magnetic surfaces and reverses its toroidal propagation direction according to plasma conditions. These observations are consistent with the interpretation that density fluctuations transported by the drift motion of plasma generate magnetic fluctuations in high-beta conditions, suggesting a similarity with the so-called entropy mode.

Keywords: innovative confinement concept, magnetospheric configuration, levitated dipole, high-beta plasma

(Some figures may appear in colour only in the online journal)

1. Section heading

The goals of the RT-1 magnetospheric configuration [1] are to understand self-organization mechanism of very high-beta

plasma in a dipole magnetic field configuration and its application to the advanced fusion concept [2]. A dipole magnetic field is the most fundamental magnetic field configuration commonly found in both in space and laboratory. The strong non-uniformity of dipole magnetic field leads to various interesting nonlinear phenomena. Plasmas confined in the steep magnetic gradients of the dipole field exhibit unique stable properties. Spontaneous formation of high-beta plasma has been observed in both planetary magnetospheres [3–5] and laboratory plasmas [6, 7]. Fluctuation-induced transport effects play crucial roles in the formation process of plasma structures. Such fluctuation effects often drive the diffusion of

* Author to whom any correspondence should be addressed.



Original content from this work may be used under the terms of the [Creative Commons Attribution 4.0 licence](https://creativecommons.org/licenses/by/4.0/). Any further distribution of this work must maintain attribution to the author(s) and the title of the work, journal citation and DOI.

plasmas, leading to the decrease of density gradients (flattening) in the confinement region. However, in the dipole magnetic field, the density flattening is realized in the phase space (density per flux tube is constant in an equilibrium state), which results in the formation of a structure with a peak in a strong magnetic field region [8, 9]. Successful formation of stable high-beta structures in the dipole field configuration have been realized in RT-1 [1, 10–14] and LDX [7, 15]. Efficient radial transport and structure formation in the dipole magnetic field of RT-1 are driven by low-frequency fluctuations on the order of kHz, which is comparable to the toroidal precession frequency of particles. In previous studies in RT-1, low-frequency fluctuations were simultaneously observed with the modification of the density structure ('reconstruction') from flattened to peaked profiles [13]. In this process, a density flattening caused by a rapid neutral gas injection is subsequently followed by the reformation of a high-beta state peaking toward the strong magnetic field region. During the reconstruction phase of the high-beta peaked structure, low-frequency fluctuations with distinguishable frequency peaks near the diamagnetic drift frequency were continuously observed [14]. Although these fluctuations have been mainly measured using magnetic probes (Bdot probes) positioned in the peripheral region of the experiment, similar fluctuations were also observed with interferometry and spectroscopy measurements. Additionally, it has been suggested that mechanical structures placed inside or near the plasma influenced the behavior of low-frequency fluctuations. For further understanding of the nature of these fluctuations and related transport phenomena in the entire plasma region, it is crucial to elucidate the spatial structure of fluctuations within the plasma.

In this study, we focus on the spatial structure and conditions of occurrence of electrostatic and magnetic fluctuations in RT-1. In addition to the Bdot magnetic probes, we introduced movable Langmuir probes capable of operating in high-heat flux region of the plasma, aiming to understand the internal structure of fluctuations in comparison with the nature of magnetic fluctuations. These measurements are expected to provide new insights into self-organization processes of the high-beta plasma in the dipole field configuration suitable for the advanced fusion concept. Previous study suggested that large mechanical structure affects the behavior of fluctuations when they are placed close to or inside the plasma. To minimize perturbations, we removed the mechanical structures of an ICH (Ion cyclotron resonance heating) antenna [12] located in the high field region of the experiment for this study. In the following sections, we will describe the experimental setup in the RT-1 device, measurement methods including the newly introduced movable Langmuir probe, and experimental results including the spatial structures and occurrence conditions of the low-frequency fluctuations.

2. Experimental setup and diagnostics

Figure 1 schematically illustrates the structure and measurement system of the RT-1 device [16]. Inside the

vacuum chamber, a high-temperature superconducting coil magnet with Bi-2223 tapes carries a permanent current of 250 kA and is magnetically levitated, in order to minimize perturbations to the plasma. The coil levitation is achieved using the attractive force generated between the feedback-controlled lifting coil magnet (28.8 kA), located on the upper part of the vacuum vessel. During magnetic levitation experiments, a magnetic field configuration with a separatrix (bold lines) is generated, as shown with thin lines in figure 1(a). By mechanically supporting the superconducting coil with an elevator, we can also generate plasmas in a pure dipole magnetic field configuration.

Plasma heating is performed with electron cyclotron resonance heating (ECH) using 2.45 GHz microwave with a maximum power of 20 kW. As suggested with the x-ray measurements, the plasma pressure of RT-1 is primarily due to the high-temperature electron component generated by ECH. This leads to the creation of plasmas with local beta values reaching up to 100% near the pressure peak [11] according to numerical Grad-Shafranov analysis of the plasma pressure profiles [17]. Here we define the local beta β_{local} as the maximum beta value in the confinement region, which is typically located on the equator between $R = 50$ and 65 cm. The measurement system of RT-1 includes microwave interferometers, x-ray detection with pulse height analysis, an x-ray CCD camera [18, 19], several spectroscopic diagnostics, and a Thomson scattering system. The discharge duration of RT-1 is on the order of one second, which is similar to the timescale of the evolution of low-frequency fluctuations. To investigate the relatively long-term behavior of electrostatic fluctuations, Langmuir probes with large stainless-steel electrodes were introduced, which enabled measurements inside the high-beta plasmas. The probe tip had a cylindrical shape with a diameter of 13 mm and a length of 12 mm. We measured the floating potential of the probe by grounding the probe tip to the chamber with a 10 M Ω resistor. We confirmed that these Langmuir probes can measure electrostatic fluctuations at the probe electrodes with a flat frequency response up to 30 kHz. In addition to two movable Langmuir probes on the equator (the vertical position of the superconducting magnet) of the experiment, an array of Langmuir probe was installed from the bottom of the chamber. The latter consisted of four probe tips placed with an azimuthal distance of 30 mm each. For the measurement of magnetic fluctuations in vertical direction (close to B_{\parallel}), we used a magnetic probe (Bdot probe) made of insulated copper winding with 20 turns and a diameter of 13 mm. The signals from the magnetic probes were amplified with a gain of 10 and then recorded as a magnetic fluctuation signal by the digitizer.

3. Spatial structure of plasmas

Figure 2 shows the density distribution measured with Langmuir probes introduced on the equatorial plane at $Z = 0$ cm and from the lower port of the chamber at $R = 72$ cm. Without the coil levitation, i.e. when the coil was placed on a mechanical support structure at $Z = 0$ cm, relatively flat density distributions were generated. Finite plasma density

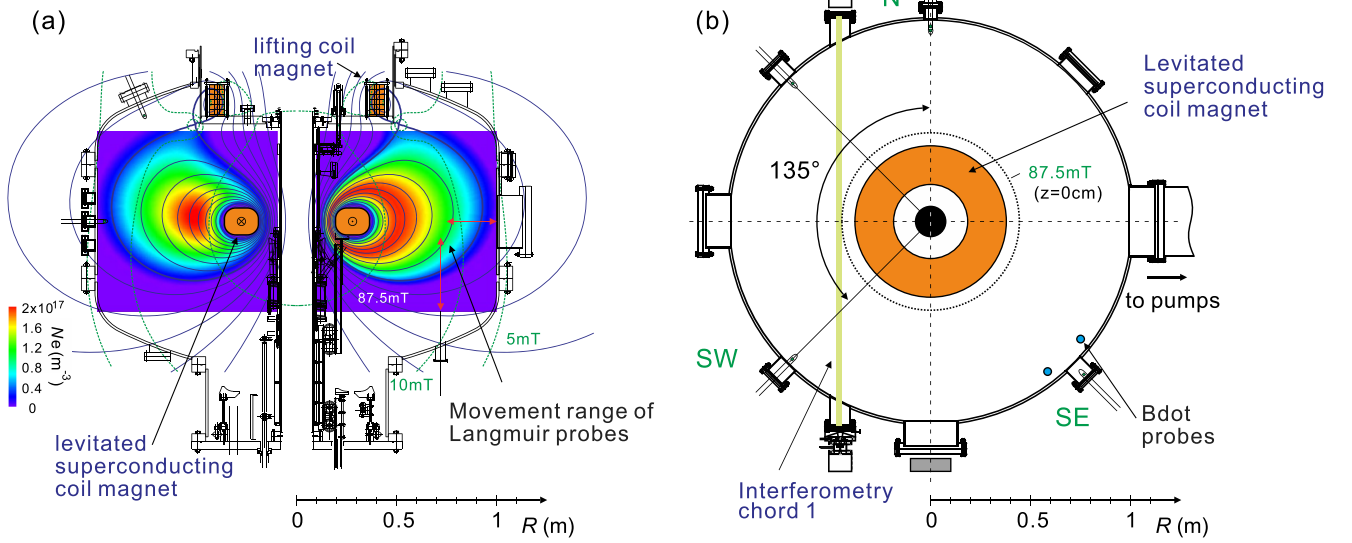


Figure 1. (a) Cross-sectional and (b) top-view diagrams of the magnetically levitated dipole, ‘artificial magnetosphere’ plasma experiment device RT-1 including diagnostics. Color contours in (a) show electron density profiles (left) before gas puffing and (right) just after the gas puffing estimated from interferometer data (see text in section 4).

was measured in a region close to the vacuum vessel wall, indicating that the wall worked as a kind of a limiter. In contrast, during coil levitation, significant density gradients were generated inside or near the separatrix. These trends are basically consistent with the density distribution reconstruction results obtained through interferometry [13]. In the coil levitation operation, low-density plasma was observed to be distributed even outside the separatrix. Measurements with Langmuir probes placed at different toroidal positions showed relatively good agreement, as shown in figure 2(a), indicating that the plasma exhibits good toroidal symmetry. The introduction of the Langmuir probes up to a few centimeters from the separatrix had a minimal impact on the line integrated density and diamagnetic signal of plasmas. When these Langmuir probes were further inserted inside the separatrix, as shown in figure 2(b), the insertion effects were no longer negligible. When the probe was placed at $Z = -15$ cm, the diamagnetic signal decreased by approximately 30%; The diamagnetic signal when the probe was located at $Z_{\text{probe}} = -40$ cm was $\Phi = 0.89$ mWb, and decreased to $\Phi = 0.62$ mWb when $Z_{\text{probe}} = -10$ cm.

Figure 3 shows the floating potential and electron temperature measured at the equator ($Z = 0$ cm plane) of the device. The Langmuir probes apparently measured the low-temperature bulk component of electrons. Within the measurable region of the plasma, the electron temperature is approximately $k_B T_e = 10$ eV or lower, and gradually increasing inward. By using the relationship between the floating potential V_f and the plasma potential V_p ,

$$V_p = V_f + \frac{k_B T_e}{e} (3.3 + 0.5 \ln \mu)$$

where μ is the normalized ion mass with respect to hydrogen [20], the radial electric field strength is estimated to be less than 100 V m^{-1} . The $E \times B$ drift velocity in the measured

range is on the order of km/s, which is one order of magnitude smaller than the grad B and curvature drift velocity. In the evaluation of drift velocities, at least in the peripheral region, the electric field does not play a significant role. This may not be the case for electric fields in the higher-density core region of the plasma, which are beyond the scope of the present study with the Langmuir probe measurements.

4. Electrostatic and electromagnetic nature of low-frequency fluctuations

In RT-1, low-frequency fluctuations with two distinguishable frequency peaks have been observed in high-beta plasma during the reconstruction phase of the spatial structures [14]. Experimentally, typical procedures to induce these low-frequency fluctuations are as follows. In the high-beta operation of RT-1, a peaked density structure is spontaneously generated, as shown in the left side of figure 1(a). The density profile is realized by using additional neutral gas puffing. The color contours in the right side of figure 1(a) show the modified rather flattened profile in this phase. Subsequently, a peaked structure is gradually formed again in the strong magnetic field region through inward transport. During this profile reconstruction process, low-frequency fluctuations with multiple frequency peaks are observed. According to magnetic fluctuation measurements, fluctuations with distinct frequency peaks appeared only when two conditions are met: first, perturbation to the plasma caused by the mechanical support structures for the superconducting coil is minimized by the coil levitation. Secondly, density reconstruction must be induced by the additional gas puffing during the discharge [13]. These fluctuation activities of the plasma were simultaneously measured using Langmuir probes and Bdot probes. The frequency spectra of electrostatic fluctuations measured by a

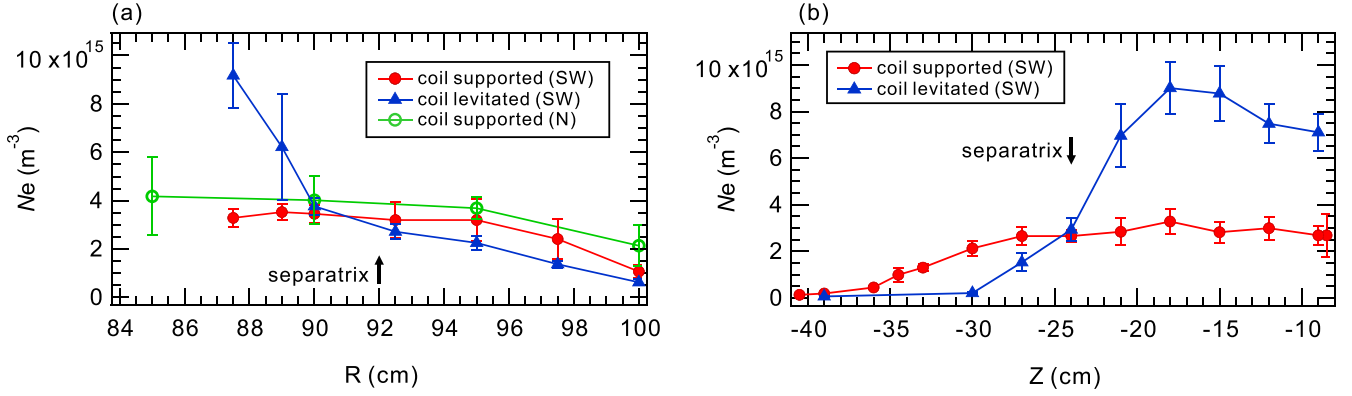


Figure 2. Electron density distribution measured with (triangles) and without (circles) coil levitation and without levitation (mechanically supported, circles), using Langmuir probes introduced (a) on the equatorial plane and (b) from the lower part of the device at $R = 72$ cm. Density profiles measured at the southwest (SW) and north (N) ports are shown in (a) for comparison.

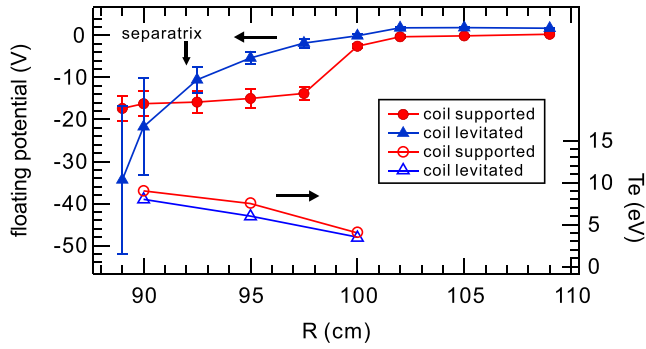


Figure 3. The radial distribution of floating potential and electron temperature measured on the equator ($Z = 0$ cm).

Langmuir probe placed at $R = 97.5$ cm and magnetic field signals measured by a Bdot probe at $R = 99$ cm were compared for cases with and without gas puffing.

Figures 4 and 5 compare the (a) electrostatic and (b) magnetic fluctuations with and without additional gas puffing. The 2.45 GHz ECH power was 15 kW for the both cases, and the maximum local beta value (before gas puffing) was approximately 15%. In figure 4, the gas puffing was conducted at $t = 1.16$ s in order to induce density reconstruction. The panels show (1) the power spectral density (PSD) during plasma discharge and (2) the time evolution of PSD. During the reconstruction phase of the electron density, magnetic fluctuations with frequency peaks around 1 kHz and 0.7 kHz were dominant, as shown in figure 4(b). While the major fluctuation component was a mode peaked at 1 kHz, difference between the intensity of modes at 1 kHz and 0.7 kHz were considerably smaller especially when the plasma has steep density profiles. The PSD of the electrostatic fluctuations in figure 4(a) showed basically similar tendency to that of magnetic fluctuations in figure 4(b). In figure 5, (a) electrostatic and (b) magnetic fluctuations were measured without conducting additional gas puffing during discharge. Although no clear frequency peaks

originated from plasma activities have been observed in the magnetic signals in this condition, electrostatic fluctuations with frequency peaks at dominant 0.7 kHz and weaker 1 kHz were found by the Langmuir probe measurements as shown in the figure.

Figure 6 plots the intensity and frequency of electrostatic and magnetic fluctuations as a function of diamagnetic signal and local beta values with additional gas puffing during discharge. The diamagnetic signals were measured with coil loops wound on the vacuum chamber at $R = 102$ cm. According to the numerical analysis of Grad-Shafranov equation for plasmas in RT-1 [17], we found that both the maximum local beta and volume integrated beta values have linear relationships with the diamagnetic signal Φ . The maximum local beta value when $\Phi = 1$ mWb is $\beta_{\text{local}} = 18\%$ in the present experimental conditions. As shown in figure 6(a), electrostatic fluctuations always had clear peaks at both 0.7 kHz and 1 kHz. In contrast, the intensity of magnetic fluctuations strongly depends on the beta value of plasma. The signal level of magnetic fluctuations at both 0.7 and 1 kHz was below the detection limit when the diamagnetic signal was below 0.6 mWb in low-beta conditions. For higher beta operations, the magnetic fluctuation component rises steeply, exhibiting the electromagnetic nature of the fluctuation. These observations implies that the rather steady electrostatic fluctuations are transformed into stronger fluctuations with a clear magnetic component in the density reconstruction phase of high-beta plasmas. The transition from electrostatic to electromagnetic modes is a phenomenon observed in many plasma experiments [21–23]. In the present study, it is considered that the propagating drift motion of density inhomogeneity of plasma produced magnetic field fluctuations in high beta conditions. As shown in figure 6(b), the observed frequency peaks do not show a strong dependence on plasma pressure but has a tendency of lower frequency for high-beta conditions. Such dependence may partly be explained by the variation of drift velocity according to the plasma conditions.

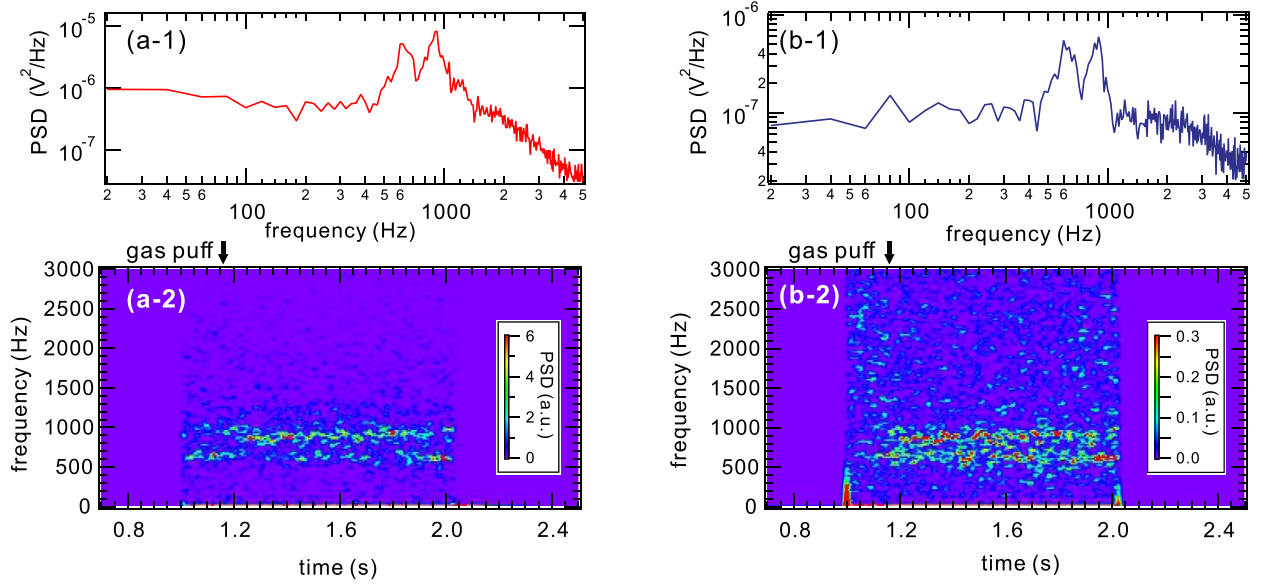


Figure 4. Electromagnetic fluctuation activities of plasma that appeared by additional gas puffing. The power spectral density (PSD) and spectrogram of fluctuations observed by (a) a Langmuir probe and (b) a magnetic probe with gas puffing at $t = 1.16$ s during the discharge. Fluctuations with clear two peaks appeared in both electrostatic and magnetic fluctuations of the plasma.

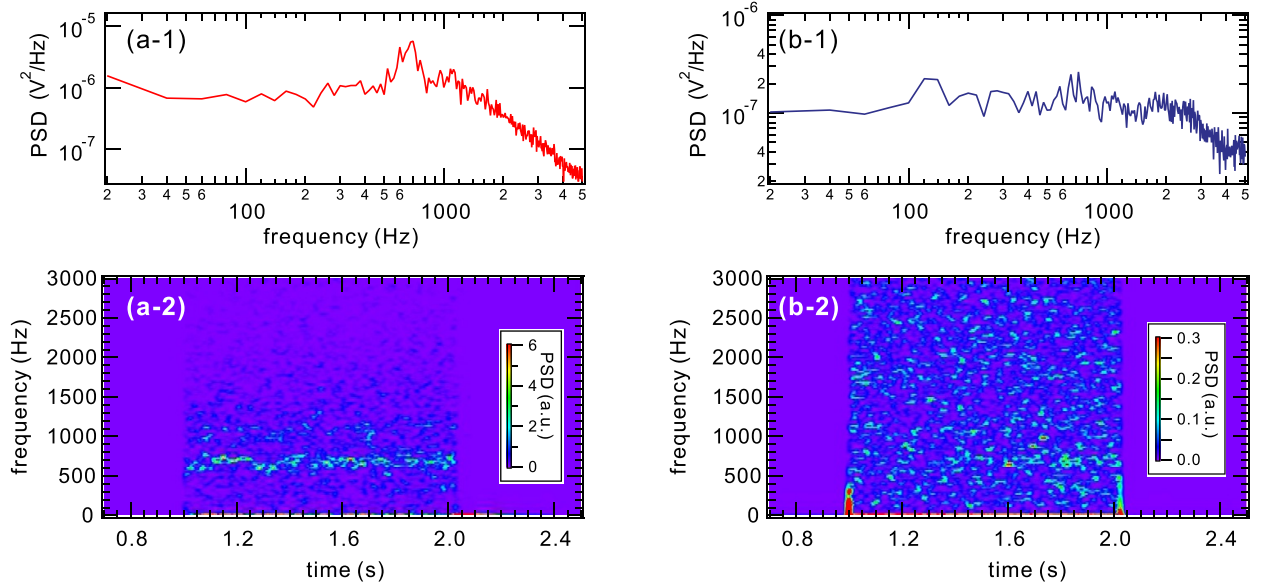


Figure 5. Electrostatic fluctuation activities of plasma observed without additional gas puffing. PSD and spectrogram of fluctuations without additional gas puffing, measured with (a) Langmuir probe and (b) magnetic probe. In the absence of gas puffing, only electrostatic fluctuations were dominant and have a peak at 0.7 kHz. No clear peaks were found in magnetic fluctuations.

5. Spatial structures of fluctuations in low- and high-beta conditions

The spatial structures of the coherent fluctuation modes with peaks around 1 kHz and 0.7 kHz were investigated with multi-point electric and magnetic measurements, and were compared for high and low beta cases. For electric and magnetic measurements, we used vertically movable Langmuir probes at $R = 72$ cm, radially movable Langmuir probes on the equator, and magnetic probes (Bdot probes) at $R = 99$ cm on the equator, respectively. The phase difference of the fluctuations

was calculated from the cross-spectrum of fluctuation signals between two measurement points separated in the toroidal direction for the estimation of propagation direction and toroidal mode number. In order to eliminate the influence of structures placed near the confinement region of the plasma, the ICH (ion cyclotron heating) antenna installed on the strong magnetic field region was removed for fluctuation measurements in these measurements. In the experiments described in this chapter, low beta plasma was generated using 10 kW of ECH, with the diamagnetic signal being 0.43 mWb (corresponding to a local beta of $\beta_{\text{local}} = 8\%$). Under high beta conditions,

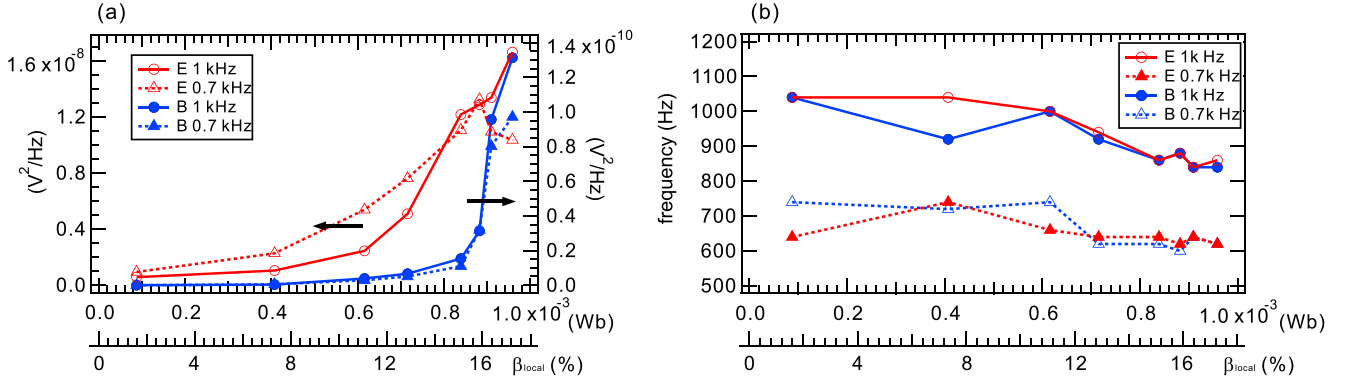


Figure 6. (a) Fluctuation intensity of electrostatic and magnetic components at 0.7 kHz and 1 kHz, and (b) the peak frequency values, both of which are shown for different diamagnetic signal values and corresponding maximum local beta values.

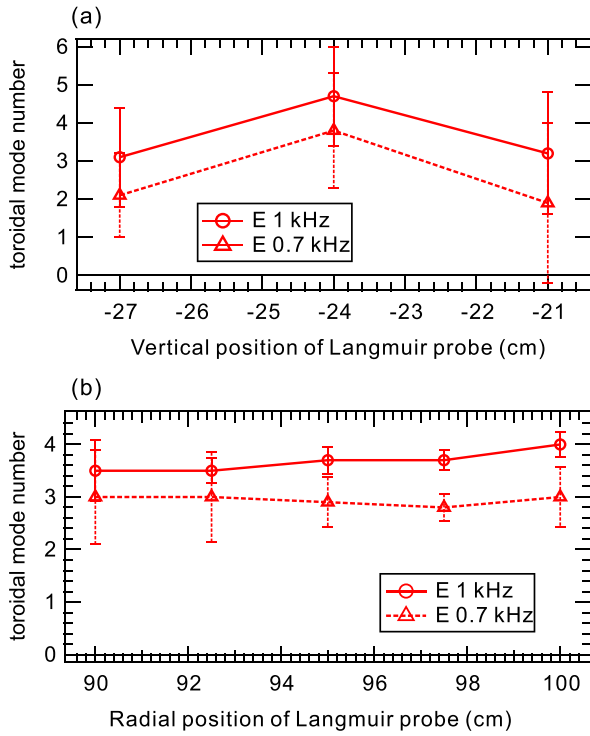


Figure 7. Toroidal mode numbers of 0.7 kHz and 1 kHz fluctuation modes obtained from measurements with Langmuir probes positioned (a) at the bottom of chamber at $R = 72$ cm and (b) in the peripheral region on the equator for low beta cases. Positive mode numbers correspond to the toroidal phase velocity in the electron diamagnetic direction.

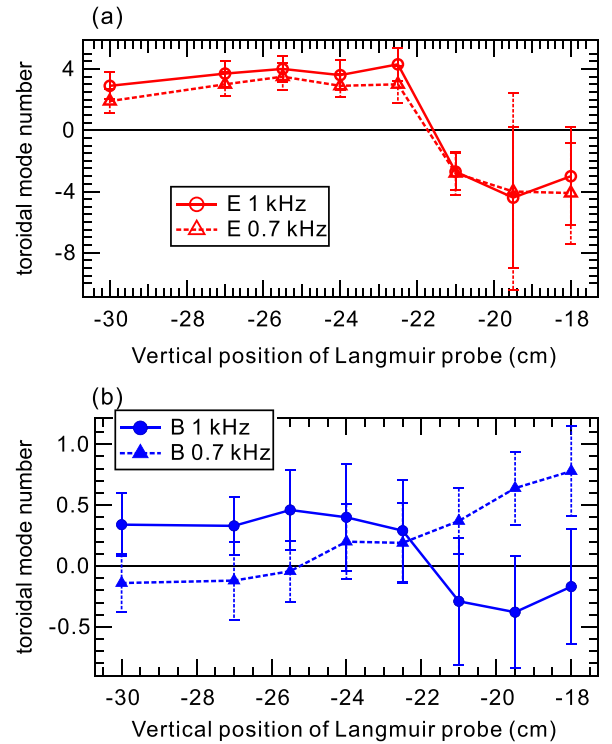


Figure 8. Phase difference of (a) electrostatic and (b) magnetic fluctuations for high beta cases. Positive mode numbers correspond to the toroidal phase velocity in the electron diamagnetic direction. The measurements were conducted with (a) vertically movable Langmuir probes at $R = 72$ cm and (b) Bdot probes at $R = 99$ cm (see main text).

plasma was generated using 17 kW of ECH, with the diamagnetic signal and corresponding local beta being 0.86 mWb and $\beta_{\text{local}} = 16\%$, respectively. In the fluctuation data plots shown in figures 7 and 8, electrostatic fluctuations are indicated with red markers, and magnetic fluctuations with blue markers. Circles and triangles show the modes peaked at 1 kHz and 0.7 kHz, respectively.

For the cases of low beta, where only electrostatic fluctuations were observed, figure 7(a) shows the toroidal mode number measured using a movable Langmuir probe introduced from the bottom of the chamber at the radial position of

$R = 72$ cm. The probe forms an array, and the mode number was estimated using measurement data from probes separated by 7.2° in the toroidal direction. The fluctuations, including both the 1 kHz and 0.7 kHz components, propagated in the electron diamagnetic direction (counterclockwise direction in the top view of the device), and the toroidal mode number was estimated to be between 2 and 4. Under low beta conditions, two additional Langmuir probes were introduced into the plasma at a position 90° away in the toroidal direction on the equatorial plane, also for phase difference measurements, see figure 7(b). In the peripheral region of the plasma, the

electrostatic fluctuations had a toroidal mode number of about 3–4, and the propagation direction was also in the electron diamagnetic direction. The measured toroidal mode numbers from both probes were similar within the error bars, although those in figure 7(a) are large mainly due to the relatively small probe spacing in measurements from the lower port. This indicates that the radial dependence of the angular velocity of toroidal propagation of electrostatic fluctuations in low beta plasma is small, and the fluctuations propagate in a rigid rotating like manner. Using the measured toroidal mode numbers of 3 (0.7 kHz) and 4 (1 kHz) at $R = 100$ cm in figure 7(b), the phase velocities of the 0.7 kHz and 1 kHz fluctuations are calculated to be 1.5 km s^{-1} and 1.6 km s^{-1} , respectively. During the occurrence of these electrostatic fluctuations, coherent fluctuations were observed also in the measurements with a microwave interferometer. As shown in figure 1(b), because the interferometer integrated the data at different radial positions along the line of sight, it can be said that the measurement results are consistent with the rigid rotating behavior of the fluctuations observed by the probe measurements. However, it should be noted that the fluctuation measurements by the Langmuir probes were not conducted throughout the entire confinement region. Depending on the spatial structure of the fluctuation intensity, coherent modes may appear in the interferometer even if the propagation of the fluctuations is not rigid body-like.

Next, the spatial structures of fluctuations in the high beta conditions were investigated, where the fluctuations showed electromagnetic behavior. Figure 8(a) shows the toroidal mode number of the fluctuations observed by the movable Langmuir probes introduced from the bottom of the chamber at $R = 72$ cm. When the movable probe was outside the separatrix ($Z > -24$ cm), the propagation direction of the electrostatic fluctuations was in the electron diamagnetic direction, the same as in the low beta case. The toroidal mode number was approximately 3, which also showed relatively good agreement with the low beta case. When the movable probes were inserted into the plasma, a reversal in the propagation direction of the fluctuations was observed. There was no significant change in the absolute values of the mode number and phase velocity, showing only a reversal in the propagation direction, as shown in the figure. Additionally, figure 8(b) shows the phase information of the magnetic field fluctuations observed in the peripheral region when the vertical position of the Langmuir probe was changed under the same conditions. The position of the magnetic probe (Bdot probe) was fixed at $R = 99$ cm on the equator. Unlike the electrostatic fluctuations, the behavior of the 1 kHz and 0.7 kHz components of the magnetic fluctuations showed clear differences. The 1 kHz component showed a similar tendency to the electrostatic fluctuations, with a reversal in the propagation direction observed as the movable Langmuir probe passed through the separatrix. On the other hand, the 0.7 kHz magnetic mode showed a relatively slow propagation velocity when the Langmuir probe was outside the separatrix. With the insertion of the probe structure inside the separatrix, it showed a clear finite toroidal mode number propagating in

the electron diamagnetic direction, which was the opposite tendency to the 1 kHz magnetic mode. Moreover, the toroidal mode numbers measured at $R = 72$ cm and in the peripheral region at $R = 99$ cm did not match and were smaller outside, suggesting that high beta plasma does not have the rigid-rotating fluctuation structure that was observed in low beta plasma.

The reversal in the propagation direction observed in the electrostatic and magnetic field fluctuations shows similarity to the fluctuations of density and temperature known as the entropy mode [24–27] or drift-temperature-gradient mode [28, 29]. In a dipole magnetic field, good confinement is achieved even in the bad curvature regions due to the compressibility effect of the plasma. According to kinetic theory, the stability limit determined by the pressure gradient exhibits different characteristics depending on the distribution of electron density and temperature, which is not distinguished in magnetohydrodynamic (MHD) theory. For plasmas with cold ions and warm electrons, which is a case for the ECH experiments at RT-1, Kesner [28, 29] showed that the stability limit is determined according to the ratio of the temperature and density gradients $\eta = d \ln T / d \ln n$. It is predicted that for $\eta > 2/3$, the entropy mode propagates in the electron diamagnetic drift direction, while for $\eta < 2/3$, the propagation direction reverses. In LDX, Garnier and coworkers [15] investigated the reversal in the phase velocity of fluctuation propagation through pellet injection experiments. The observed reversal in the toroidal propagation velocity in RT-1 can be caused by the variation of the internal temperature and density profiles of the plasma realized by the introduction of the Langmuir probe structure.

6. Summary

In this study, we report the progress of experimental studies conducted at the RT-1 levitated dipole on plasma fluctuations related to transport and structure formation in a dipole magnetic field configuration. Regarding low-frequency fluctuations that appear during the structure formation phase, our observations revealed that (1) the electromagnetic fluctuation mode at high- β states was excited as an electrostatic mode for low- β plasmas, (2) this wave propagated in the toroidal direction with a mode number of 3 or 4 according to multi-point electrostatic measurements, and (3) the wave propagation changed its toroidal direction depending on plasma parameters.

Acknowledgments

The authors thank Y. Yokota, S. Murai, K. Takeda, Z. Wen, and K. Mimura for their contribution to the experiments and discussions. This work was supported by JSPS KAKENHI Grant Nos. 17H01177, 22H04936, and 22H00115, the NIFS Collaboration Research Program Nos. NIFS22KIPR008 and NIFS22KINR001.

ORCID iDs

H. Saitoh  <https://orcid.org/0000-0001-8457-5570>
 M. Nishiura  <https://orcid.org/0000-0002-2752-3333>
 N. Kenmochi  <https://orcid.org/0000-0003-1088-8237>
 N. Sato  <https://orcid.org/0000-0002-2973-0635>

References

- [1] Yoshida Z., Ogawa Y., Morikawa J., Watanabe S., Yano Y., Mizumaki S., Tosaka T., Ohtani Y., Hayakawa A. and Shibui M. 2006 First plasma in the RT-1 device *Plasma Fusion Res.* **1** 008
- [2] Hasegawa A. 1987 A dipole field fusion reactor *Plasma Phys. Control. Fusion* **11** 147
- [3] Schulz M. and Lanzerotti L.J. 1974 *Particle Diffusion in the Radiation Belts* (Springer)
- [4] Brice N. and McDonough T.R. 1973 Jupiter's radiation belts *Icarus* **18** 206
- [5] Chen Y., Geoffrey D.R. and Reiner H.W.F. 2007 The energization of relativistic electrons in the outer Van Allen radiation belt *Nat. Phys.* **3** 614
- [6] Yoshida Z., Saitoh H., Yano Y., Mikami H., Kasaoka N., Sakamoto W., Morikawa J., Furukawa M. and Mahajan S.M. 2013 Self-organized confinement by magnetic dipole: recent results from RT-1 and theoretical modelling *Plasma Phys. Control. Fusion* **55** 014018
- [7] Boxer A.C., Bergmann R., Ellsworth J.L., Garnier D.T., Kesner J., Mauel M.E. and Woskov P. 2010 Turbulent inward pinch of plasma confined by a levitated dipole magnet *Nat. Phys.* **6** 207
- [8] Yoshida Z. 2016 Self-organization by topological constraints: hierarchy of foliated phase space *Adv. Phys.* **X** 1 2
- [9] Sato N. and Yoshida Z. 2018 Diffusion with finite-helicity field tensor: a mechanism of generating heterogeneity *Phys. Rev. E* **97** 022145
- [10] Kawazura Y., Yoshida Z., Nishiura M., Saitoh H., Yano Y., Nogami T., Sato N., Yamasaki M., Kashyap A. and Mushiaki T. 2015 Observation of particle acceleration in laboratory magnetosphere *Phys. Plasmas* **22** 112503
- [11] Nishiura M., Yoshida Z., Saitoh H., Yano Y., Kawazura Y., Nogami T., Yamasaki M., Mushiaki T. and Kashyap A. 2015 Improved beta (local beta > 1) and density in electron cyclotron resonance heating on the RT-1 magnetosphere plasma *Nucl. Fusion* **55** 053019
- [12] Nishiura M. *et al* 2017 Ion cyclotron resonance heating system in the RT-1 magnetospheric plasma *Nucl. Fusion* **57** 086038
- [13] Nishiura M., Yoshida Z., Kenmochi N., Sugata T., Nakamura K., Mori T., Katsura S., Shirahata K. and Howard J. 2019 Experimental analysis of self-organized structure and transport on the magnetospheric plasma device RT-1 *Nucl. Fusion* **59** 096005
- [14] Kenmochi N., Yokota Y., Nishiura M., Saitoh H., Sato N., Nakamura K., Mori T., Ueda K. and Yoshida Z. 2022 Inward diffusion driven by low frequency fluctuations in self-organizing magnetospheric plasma *Nucl. Fusion* **62** 026041
- [15] Garnier D.T., Mauel M.E., Roberts T.M., Kesner J. and Woskov P.P. 2017 Turbulent fluctuations during pellet injection into a dipole confined plasma torus *Phys. Plasmas* **24** 012506
- [16] Ogawa Y., Yoshida Z., Morikawa J., Saito H., Watanabe S., Yano Y., Mizumaki S. and Tosaka T. 2009 Construction and operation of an internal coil device, RT-1, with a high-temperature superconductor *Plasma Fusion Res.* **4** 020
- [17] Furukawa M. 2014 Effects of pressure anisotropy on magnetospheric magnetohydrodynamics equilibrium of an internal ring current system *Phys. Plasmas* **21** 012511
- [18] Liang Y., Ida K., Kado S., Minami T., Okamura S., Nomura I., Watanabe K.Y. and Yamada H. 2001 Photon-counting CCD detector as a tool of x-ray imaging *Rev. Sci. Instrum.* **72** 717
- [19] Saitoh H., Yano Y., Mizushima T., Morikawa J. and Yoshida Z. 2009 Initial results of x-ray imaging and energy spectrum measurements of hot electron plasmas in RT-1 *Plasma Fusion Res.* **4** 050
- [20] Hershkovitz N. 1989 *How Langmuir Probes Work* (Academic) pp 113–83
- [21] Degeling A.W., Borg G.G. and Boswell R.W. 2004 Transitions from electrostatic to electromagnetic whistler wave excitation *Phys. Plasmas* **11** 2144
- [22] Spagnolo S., Zuin M., Cavazzana R., Martinez E., Patelli A., Spolaore M. and Colasuonno M. 2016 Characterization of electromagnetic fluctuations in a HiPIMS plasma *Plasma Sources Sci. Technol.* **25** 065016
- [23] Razzak M.A., Kondo K., Uesugi Y., Ohno N. and Takamura S. 2004 Transition from electrostatic-to-electromagnetic mode in a radio-frequency Ar inductively coupled plasma in atmospheric pressure *J. Appl. Phys.* **95** 427
- [24] Kadomtsev B.B. 1960 Convective pinch instability *Sov. Phys. JETP* **10** 780
- [25] Ricci P., Rogers B.N., Dorland W. and Barnes M. 2006 Gyrokinetic linear theory of the entropy mode in a Z pinch *Phys. Plasmas* **13** 062102
- [26] Kobayashi S., Rogers B.N. and Dorland W. 2010 Particle pinch in gyrokinetic simulations of closed field-line systems *Phys. Rev. Lett.* **105** 235004
- [27] Qian L., Wang Z., Li J. and Wang X. 2020 Entropy modes in multi-component plasmas confined by a dipole field *Phys. Plasmas* **27** 042104
- [28] Kesner J. 2000 Interchange modes in a collisional plasma *Phys. Plasmas* **7** 3837
- [29] Kesner J. 2002 Electrostatic drift modes in a closed field line configuration *Phys. Plasmas* **9** 3895